all-*trans*-Retinal Forms a Visible-Absorbing Pigment with Human Rod Opsin[†]

Lioubov I. Brueggemann and Jack M. Sullivan*

Department of Ophthalmology, State University of New York, Upstate Medical University, Syracuse, New York 13210

Received September 26, 2000; Revised Manuscript Received January 10, 2001

ABSTRACT: Rhodopsin activation elicits transmembrane currents due to electrostatic events associated with conformational changes. We employed the sensitive rhodopsin early receptor current approach to reevaluate whether all-*trans*-retinal can form a visual pigment with rod opsin apoprotein. An opsin shift above 440 nm is induced in the action spectrum of charge motions caused by visible flashes in cells expressing human rod opsin and regenerated with all-*trans*-retinal, compared to cells without opsin. Near-ultraviolet stimulation of opsin regenerated with all-*trans*-retinal promotes charge motions similar to those arising from the meta-II signaling state while photochemically regenerating a pigment with ground state charge motion properties. These results indicate that all-*trans*-retinal can form a visual pigment with opsin, through both protonated and unprotonated Schiff base linkages and likely within the native ligand binding pocket at lysine-296. The agonist effects of all-*trans*-retinal may relate to its structural accommodation within the core of opsin, similar to other G-protein-coupled receptors.

Covalent binding of 11-*cis*-retinaldehyde to lysine-296 in the ligand binding pocket of opsin results in the protonated Schiff base (PSB)[1] retinylidene chromophore (retinal$-_{15}$C$=$N$^+$H$-$opsin) of rhodopsin, the rod photoreceptor visual pigment (*1*−*3*). An all-*trans*-retinylidene chromophore with either protonated (bathorhodopsin$_{538nm}$ → lumirhodopsin$_{497nm}$→ metarhodopsin-I$_{478nm}$) or unprotonated (metarhodopsin-II: meta-II$_{380nm}$) covalent Schiff base (SB) linkages occupies the ligand binding pocket after initial photochemical *cis*-to-*trans* isomerization during bathorhodopsin formation and during all subsequent thermal intermediates leading to the biochemically active state(s) of meta-II$_{380nm}$ (*2*). In addition, all-*trans*-retinal is a pharmacological agonist for the opsin apoprotein receptor leading to a ligand-associated conformational state(s) which activate(s) the G-protein, transducin, in both membranes and detergent extracts (*4*−*8*). These results suggest that the opsin apoprotein might be able to accommodate the all-*trans*-retinal ligand into its binding pocket. However, a light-absorbing pigment due to all-*trans*-retinal reaction with rod opsin has never been detected by absorption spectrophotometry in either intact disk membranes or detergent extracts, resulting in a model that all-*trans*-retinal achieves its effects through a noncovalent complex with the opsin apoprotein (*9*, *10*). We have recently developed an especially sensitive approach, the early receptor current (ERC), to study the conformational biophysical of expressed rhodopsin pigments (*11*, *12*). The ERC reflects electrically-active conformational dynamics of rhodopsin oriented in a membrane plane during the forward bleaching pathway or during photochemical conversion from the biochemically active meta-II$_{380nm}$ state(s). The ERC can be used to measure rhodopsin charge motions from as little as 10^6 molecules in single live cells and is thus several orders of magnitude more sensitive than absorption spectrophotometry (*11*).

To attempt to resolve the apparent paradox between the activity of the all-*trans*-retinylidene chromophore during forward bleaching of rhodopsin and its biochemical and pharmacological effects on the bleached apoprotein, we reexplored, with the ERC approach, whether all-*trans*-retinal can form a visual pigment with the opsin apoprotein. We show that an electrically active visible-absorbing pigment results from formation of a protonated Schiff base between opsin and all-*trans*-retinal. An ultraviolet (UV)-absorbing pigment also forms to promote an inverted photocurrent through photoisomerization of opsin-bound all-*trans*-retinal and regeneration of a ground state rhodopsin. We conclude that the ligand binding pocket of human rod opsin has greater conformational adaptability than found in prior attempts to demonstrate pigment formation with all-*trans*-retinal by spectrophotometry.

MATERIALS AND METHODS

WT HEK293S cells constitutively expressing WT human opsin and parental HEK293S cells were grown, fused, and regenerated for 30 min as described (*11*). Spectrophotometrically quantified ethanolic stocks of 11-*cis*-retinal or all-*trans*-retinal were added to a final concentration of 25 μM, and 0.025% (v/v) α-D-tocopherol (vitamin E) was added as an antioxidant. The ERC signal was recorded using the patch-

[†] This work was funded by a grant from the National Eye Institute (EY11384 to J.M.S.).

* Correspondence should be addressed to this author at the Institute for Human Performance, Rm 4210, SUNY Upstate Medical University, 750 East Adams St., Syracuse, NY 13210. Telephone: (315)-464-6694. Fax: (315)-464-9942. E-mail: Sullivaj@mail.upstate.edu.

[1] Abbreviations: C_{mem}, membrane capacitance; ERC, early receptor current; fC, femtocoulomb; HEK293S, human embryonic kidney cells (suspension adapted); meta-II$_{380nm}$, metarhodopsin-II$_{380nm}$; NH_2OH, hydroxylamine; pA, picoampere; pC, picocoulomb; pF, picofarad; PSB, protonated Schiff base; Q, ERC charge in coulombs; R_1, negative component of ERC; R_2, positive component of ERC; SB, Schiff base; SE, standard error of the mean; UV, ultraviolet; WT, wild-type human opsin; WT HEK293S, HEK293S cells constitutively expressing WT human rod opsin. Single letter chemical abbreviations are used for amino acids (e.g., E = glutamate and K = lysine).

10.1021/bi002267g CCC: $20.00
Published on Web 03/15/2001

clamp whole-cell recording technique. The ERC recording setup and procedures have been extensively described previously (*11*−*13*). Patch pipets with low resistance (2−4 MΩ) were filled with (in mM) 70 tetramethylammonium hydroxide (TMA-OH), 70 2-(*N*-morpholino)ethanesulfonic acid (MES-H), 70 TMA fluoride, 10 EGTA−CsOH, and 10 HEPES−CsOH, pH 6.5 (solution I-1). The bath solution contained (in mM) 140 TMA-OH, 140 MES-H, 2.0 $CaCl_2$, 2.0 $MgCl_2$, and 5.0 HEPES−NaOH, pH 7.0 (solution E-1). To regenerate the R_1 signal, extracellular perfusion of bath solution E-1 containing 2% BSA (w/v) and 50 μM all-*trans*-retinal was followed by 30 min of dark adaptation. Extracellular perfusion of bath solution E-1 containing 10 mM hydroxylamine (NH_2OH) for 10 min followed by washout with E-1 was used to test the reactivity of the chromophores of HEK293S and WT HEK293S cells initially regenerated with all-*trans*-retinal. Since the ERC is a capacitative current, whole-cell capacitance (C_{mem}) and series resistance were measured but not electronically compensated. Cell surface area was estimated from C_{mem} (1 μF/cm^2, F in farads). Whole-cell ERC currents were recorded at 5 kHz bandwidth using an eight-pole Bessel filter and digitized at 200 μs/point. All experiments were conducted at room temperature (21−22 °C).

Photolytic flashes were controlled and ERC data acquired using pCLAMP 5.51 (CLAMPEX; Axon Industries, Foster City, CA) (*11*, *13*). Rhodopsin in giant cells was activated by a bright flash monochromatic microbeam apparatus described in detail elsewhere (*14*). For routine ERC recordings broad-band (70 nm, full width at half-maximum) three-cavity band-pass filters centered at 500 nm delivered flash intensities to the specimen plane of the microscope of 3.9 $\times$ 10^8 photons/μm^2. For broad-band (70 nm) near-UV flashes a filter centered at 350 nm was used which gave flashes at intensity 0.43 $\times$ 10^8 photons/μm^2. In action spectrum experiments 30 nm band-pass filters were used, centered at 400, 420, 440, 460, 480, 500, 520, 540, and 580 nm which delivered intensities (in units of 10^8 photons/μm^2) of 0.92 (400 nm), 1.74 (420 nm), 1.92 (440 nm), 2.59 (460 nm), 2.00 (480 nm), 2.13 (500 nm), 1.86 (520 nm), 1.38 (540 nm), and 1.09 (580 nm). To bleach the ERC charge in a cell, successive flashes were delivered until the signal was extinguished. Bleaching was followed by 10 min of dark adaptation prior to delivery of additional flash stimuli.

ERC data were analyzed using Origin (Version 4.1) (Microcal Software, Northampton, MA). Negative charge (in coulombs, C) in each ERC waveform (Q_i) was obtained by integration of negative ERC current signals after subtraction of baseline current (see Figure 1D,F). Total negative charge for bleaching (Q_∞) was obtained by summing Q_i values in a given bleaching extinction. For action spectra the integrated value of the total inward charge motion (Q_∞) was normalized to both cell size (C_{mem}), since ERC charge is linearly proportional to cell size (*11*), and the relative differences in flash intensity at each test wavelength relative to 500 nm (*12*). The mean ± standard error of the charge values are plotted versus wavelength and the data fit with a standard inverse polynomial function. A difference spectrum is obtained by subtracting the HEK293S action spectrum from that of WT HEK293S, and the positive component was fit by an inverse polynomial function to obtain peak wavelength. Nonlinear curve fitting employed a Marquardt−Levinberg nonlinear least-squares algorithm (Origin 4.1) (confidence level set >0.95). Molecular graphics models of bovine rhodopsin were obtained from the G-protein-coupled receptor database (http://swift.embl-heidelberg.de/7tm/models) and examined with WebLab Viewer (Molecular Simulations Inc., San Diego, CA).

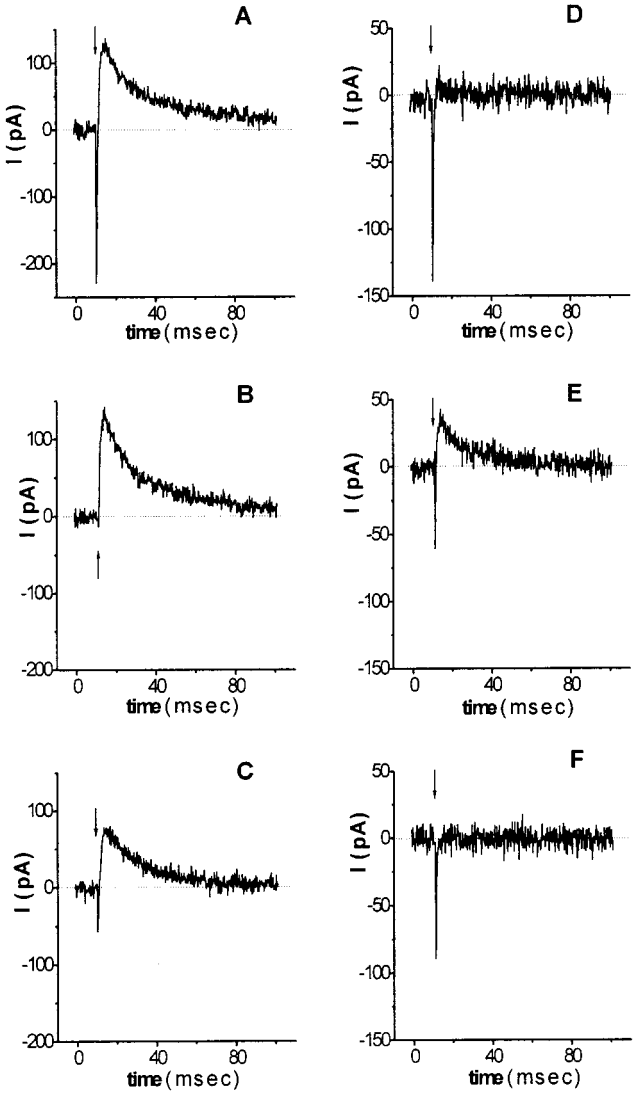

FIGURE 1: all-*trans*-Retinal regenerates an ERC activated by visible light. (A) A WT HEK293 cell (C_{mem} = 635.2 pF) was regenerated with 11-*cis*-retinal, and the ERC obtained on the first 500 nm flash is shown. The arrow indicates flash presentation, and the dotted line indicates zero current level. (B) In the same cell after bleaching and dark adaptation a 500 nm flash generated an ERC with a pure R_2 component. (C) The R_1 signal was regenerated in the same cell by extracellular perfusion of E-1 containing all-*trans*-retinal. (D) Photolysis of the WT HEK293S cell (C_{mem} = 281.3 pF) regenerated with all-*trans*-retinal resulted in a negative signal upon a 500 nm flash. (E) In the same cell after a single bleach at 500 nm, followed by dark adaptation, a 500 nm flash generated an ERC with both R_1 and R_2 components. (F) HEK293S cell (C_{mem} = 185 pF) regenerated with all-*trans*-retinal had a pure negative signal upon 500 nm flash.

RESULTS

The ERC of normal vertebrate rhodopsin has two components, the inward and rapid (R_1) current which occurs concurrent with the flash and a large outward (R_2) current which peaks on a millisecond time scale concurrent with

meta-II_{380nm} formation (*11*) (Figure 1A). These are seen following flash photolysis at 500 nm of 11-*cis*-retinal-regenerated wild-type human rhodopsin (WT) expressed in human embryonic kidney cells (WT HEK293S) (*11*). Similar signals with both R_1 and R_2 components have been previously recorded during photoactivation of rhodopsin in rod and cone photoreceptors (*15*). The outside of the cell is equivalent to the intradiscal side of a rod photoreceptor so rhodopsin is oriented outside out in the plasma membrane of WT HEK293S cells (*11*).

Following a single flash or complete extinction of the bimodal ERC at 500 nm and after dark adaptation, subsequent 500 nm flashes generate ERC signals with a pure outward R_2 component (Figure 1B). The R_2 charge motion can be bleached and has an action spectrum which is consistent with normal human rhodopsin absorbance after regeneration with 11-*cis*-retinal (*12*). This demonstrates that the pure R_2 signal represents charge motions associated with the forward bleaching path of the ground state rhodopsin pigment (*12*).

The R_1 component can be recovered in 11-*cis*-retinal-regenerated, bleached, and subsequently dark-adapted WT HEK293S cells by extracellular perfusion with a solution containing all-*trans*-retinal (Figure 1C). WT HEK293S cells initially regenerated with all-*trans*-retinal respond to 500 nm flashes with ERCs having a pure negative waveform similar in shape and kinetics to the R_1 signal found in cells initially regenerated with 11-*cis*-retinal (Figure 1D). After bleaching of the pure negative signal in all-*trans*-retinal-regenerated cells by 500 nm flashes and subsequent dark adaptation, additional flashes elicit ERCs with both R_1- and R_2-like responses on the first flash similar to those seen in WT HEK293S cells after initial regeneration with 11-*cis*-retinal (Figure 1E). A single bleach at 500 nm was sufficient to convert the pure R_1 signal intrinsic to primary all-*trans*-retinal regeneration to an ERC signal with 11-*cis*-retinal characteristics, that is, with both R_1 and R_2 components. WT HEK293S cells initially regenerated with 11-*cis*-retinal require several (*4*−*6*) flashes to extinguish the pure R_2 signal during secondary bleaches, whereas cells initially regenerated with all-*trans*-retinal require only 1−2 flashes to fully extinguish the R_2 component after bleaching of the pure R_1 signal and subsequent dark adaptation. These results indicate that all-*trans*-retinal can generate a visible light-absorbing and bleachable pigment in the WT HEK293S cell plasma membrane and that a photoconversion/thermal process can transform this pigment into one with ERC charge motion resembling an 11-*cis*-retinal-regenerated rhodopsin. The latter process, however, is less efficient and substoichiometric in comparison to primary regeneration of opsin in WT HEK293S cells with 11-*cis*-retinal. The results also suggest that the origin of the R_1 ERC component during initial flash photolysis of WT HEK293S cells regenerated with 11-*cis*-retinal may be due to the presence of a small amount of all-*trans*-retinal during the initial pigment regeneration. In fact, we have found that ethanolic stocks of 11-*cis*-retinal contain a small amount of all-*trans*-retinaldehyde when analyzed by high-pressure liquid chromotography (Dr. B. Vought, personal communication). This prompts the question as to whether the R_1 signal results, at least in part, from reaction of all-*trans*-retinal with plasma membrane opsin to generate a visible-absorbing pigment.

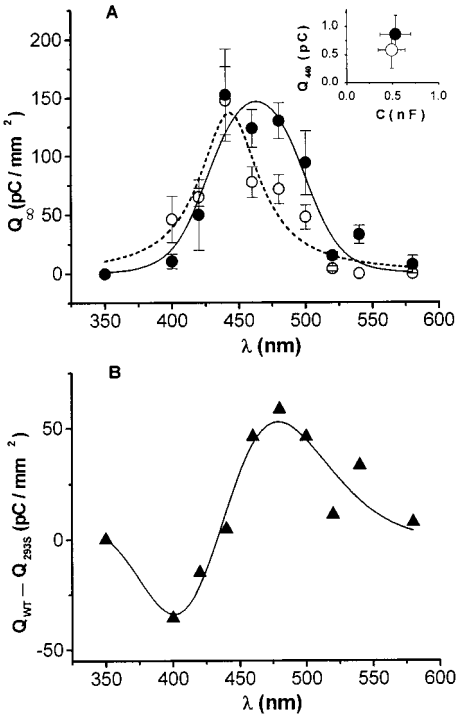

FIGURE 2: Action spectra of all-*trans*-retinal regenerated WT HEK293S and HEK293S cells. (A) The WT HEK293S cell action spectrum (●, $n = 3-11$ cells/wavelength) peaked at 463.1 ± 3.7 nm with a bandwidth (fwhm) of 107.5 ± 11.9 nm, and the HEK293S cell action spectrum (○, $n = 6-16$ cells/wavelength) peaked at 443.2 ± 3.6 nm with a bandwidth of 54.2 ± 10.4 nm. Charge motion data were normalized by each cell size (C_{mem}) and for the differences in photon delivery within the respective stimulus bands (equal photon action spectra). (Insert) Comparison of the amount of negative charge motion upon 440 nm stimulation versus C_{mem} in WT HEK293S cells (●, $n = 11$ cells) and in HEK293S cells (○, $n = 16$ cells). (B) The difference spectrum of the negative charge motion has a positive peak at 482.5 ± 6.8 nm with a bandwidth of 57.8 ± 20.7 nm.

To investigate the origin of the initially pure R_1 signal in WT HEK293S cells, large (>250 pF) fused HEK293S cells that do not express opsin were regenerated with all-*trans*-retinal. In these cells 500 nm flashes generated ERCs with a pure negative component waveform similar to the R_1 component in WT HEK293S cells (Figure 1F). The mean sizes of the fused WT HEK293S (531.9 ± 168.6 pF, mean ± standard error) and HEK293S (491.3 ± 147.1 pF) cells used in this study and the mean amplitudes of the negative R_1-like charge motion (WT, 860.0 ± 334.3 fC; 293S, 581.4 ± 329.1 fC) were not statistically different (*F* statistic, $p > 0.05$) (Figure 2A, inset). Unlike WT HEK293S cells, photolytic charge motions elicited from HEK293S cells regenerated with all-*trans*-retinal never had any positive component during flash photolysis after initial regeneration or after initial negative signal extinction and subsequent dark adaptation. The appearance of the R_2 signal requires the presence of opsin in WT HEK293S cells. To determine whether the R_1-like ERC component was influenced by opsin, action spectra of the negative component of all-*trans*-retinal-regenerated WT HEK293S and HEK293S cells were obtained (Figure 2A). The R_1-like action spectrum of HEK293S cells regenerated with all-*trans*-retinal has a maximum at 443.2 ± 3.6 nm. The origin of the negative charge motion in HEK293S cells is consistent with the visible

light absorption by a population of PSBs (peak ≈ 440 nm) (*16*), formed by reaction of all-*trans*-retinal with primary amines of plasma membrane lipids (e.g., phosphatidylethanolamine) or lysines (K) in non-opsin proteins (*17*). The action spectrum of the R_1 signal from WT HEK293S cells regenerated with all-*trans*-retinal, however, was red shifted and peaked at 463.1 ± 3.7 nm. This approximately 20 nm bathochromic shift of the action spectrum of the R_1-like charge motion in opsin-expressing WT HEK293S cells relative to HEK293S cells suggests that all-*trans*-retinal specifically reacts with plasma membrane opsin. Moreover, the action spectrum of the negative signal in WT HEK293S cells was broadened (full width at half-maximum = 107.5 ± 11.9 nm) in comparison to the more narrow spectral width in HEK293S cells (54.2 ± 10.4 nm). This may suggest that the all-*trans*-retinal (50 μM) chromophore reacts, in part, in an anisotropic environment directly associated with the opsin protein (∼2.4 μM; see ref *11*) in the plasma membrane of WT HEK293S cells. But, part of the R_1 signal in WT HEK293S cells results from the reaction of all-*trans*-retinal with non-opsin constituents of the plasma membrane that are otherwise identical to those in HEK293S cells. To separate the summed contributions of opsin and non-opsin sources to the action spectrum of the R_1 signal in WT HEK293S cells, a difference spectra was generated by subtracting the HEK293S action spectrum from the WT HEK293S spectrum. The difference spectrum has a positive maximum at 482.5 ± 6.8 nm and an amplitude 2.4 times smaller, at peak wavelength, in comparison to WT HEK293S action spectra (Figure 2B). The absolute action spectrum and the difference action spectrum of the negative ERC signal in all-*trans*-retinal-regenerated WT HEK293S cells, with respect to that in HEK293S cells, is bathochromically shifted about 20 and 42 nm beyond 440 nm, respectively. This provides strong evidence that all-*trans*-retinal forms a PSB within the opsin protein in the plasma membrane of WT HEK293S cells and in an anisotropic environment which promotes charge delocalization of the all-*trans*-retinylidene chromophore (batho shift). The opsin shift induced by the ligand binding pocket of mammalian opsins upon the 11-*cis*-retinylidene PSB chromophore is about 60 nm (440 → 500 nm) and results, in largest part, due to the $E113^-$ counterion that both neutralizes the electrostatic environment around the PSB and tunes the absorption dipole (*18*−*20*). The bathochromic shift we find with all-*trans*-retinal is not as large as in the native rhodopsin pigment but is, nevertheless, consistent with a bathochromic shift induced by the specific interaction of all-*trans*-retinal with amino acid side chains of the transmembrane helices of opsin that embrace a ligand binding pocket.

To further investigate the bathochromically shifted pigment resulting from the reaction of all-*trans*-retinal with plasma membrane opsin in WT HEK293S cells, we examined the sensitivity of the negative R_1-like charge motion to extracellular perfusion of recording buffer containing 10 mM NH_2OH which converts retinaldehydes to oxime forms (−C═NOH) that do not form visual pigments. The negative ERC seen in control HEK293S cells initially regenerated with all-*trans*-retinal does not recover following photolytic extinction even after washout of NH_2OH (data not shown). In addition, other HEK293S cells on the same coverslip subjected to ERC recording after NH_2OH perfusion and washout never had negative ERC signals. NH_2OH in the recording chamber would react rapidly with unprotected PSBs or unprotonated SBs on the extracellular surface of the HEK293S giant cells, causing a net extraction of unprotected retinals as oximes over time due to a mass action effect (*12*). In contrast, WT HEK293S cells initially regenerated with all-*trans*-retinal, stimulated once to ascertain R_1 signal presence (500 nm) and then dark adapted, generated ERCs with both R_1 and R_2 components on the first 500 nm flash after NH_2OH perfusion and washout. All subsequent 500 nm flashes on the same cell elicited ERCs with a pure R_2 component. Moreover, the same results were observed on all other cells recorded from the same coverslip (≥10 min) after NH_2OH perfusion and washout. The R_1-like charge motion always disappears after the first 500 nm flash after 10 min exposure to NH_2OH and washout. That the R_1 response to the first flash after extracellular NH_2OH perfusion/washout was decreased but not extinguished suggests that, in the dark, the opsin in WT HEK293S cells protects a fraction of chromophores that cause negative transmembrane charge motions from attack by NH_2OH. The partial loss of the R_1 signal in WT HEK293S cells due to extracellular NH_2OH is not surprising given that other non-opsin binding sites for all-*trans*-retinal are present in the plasma membrane and, as in HEK293S cells, offer no protection to chemical reaction. Once the fraction of opsin-protected all-*trans*-retinylidene pigment is bleached, presumably in association with hydrolysis of SB linkages, the negative charge motion does not recover. When all-*trans*-retinal is loaded at higher concentration (200 μM), R_1 signals are larger and remain protected from NH_2OH longer.

In addition to a pigment absorbing in the visible range all-*trans*-retinal also forms a pigment absorbing in the near-UV in WT HEK293S cells. This pigment is distinct because it generates a unique charge motion in comparison to those generated with 500 nm flashes. Flash photolysis at 350 nm of all-*trans*-retinal-regenerated WT HEK293S cells, but not HEK293S cells, induces charge motion responses with an instantaneous positive rise (≤1 μs) that is coincident with photon delivery and is immediately followed by a fast millisecond-order relaxation which crosses the zero current baseline at about 20 ms to result in a slowly relaxing inward charge motion (Figure 3A). After several successive 350 nm flashes associated with charge motion responses as in Figure 3A, normal ERCs with characteristic R_1 and R_2 components are observable upon 500 nm flashes within the few seconds necessary to convert from 350 to 500 nm flash stimulation of all-*trans*-retinal-regenerated WT HEK293S cells (Figure 3B). The presence of an R_2 signal indicates the formation of a visual pigment with a *cis*-retinylidene PSB chromophore (e.g., 9-*cis*, 11-*cis*). These data are consistent with a photochemical conversion with 350 nm flashes of an all-*trans*-retinylidene unprotonated SB chromophore to a *cis*-retinylidene PSB species. In comparison, when rhodopsin in WT HEK293S cells regenerated with 11-*cis*-retinal is completely bleached with a series of rapid 500 nm flashes and then exposed to 350 nm flashes, photoconversion ERCs (from meta-II_{380nm}) appear with a small, rapidly relaxing outward component (not well resolved but similar to the initial positive deflection and millisecond-order relaxation in all-*trans*-retinal-regenerated cells) and a slow millisecond-order negative component (Figure 3C). After successive 350

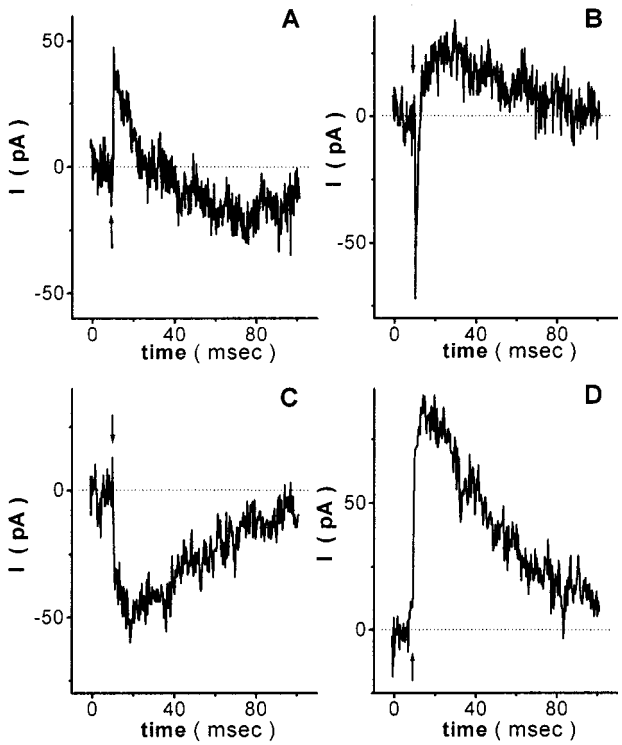

FIGURE 3: all-*trans*-Retinal regenerates a meta-II-like state. (A) ERC elicited in response to a 350 nm flash from a WT HEK293S cell (C_{mem} = 543.6 pF) regenerated with all-*trans*-retinal. The arrow indicates flash presentation, and the dotted line indicates zero current level. (B) In the same cell after three 350 nm flashes followed by a 30 s wait time, a 500 nm flash generated an ERC with both negative and positive components. (C) ERC from a WT HEK293S cell (C_{mem} = 1517 pF), regenerated with 11-*cis*-retinal, bleached at 500 nm and immediately stimulated with a 350 nm flash. (D) In the same cell after three 350 nm flashes followed by a 30 s wait, a 500 nm flash elicited a pure positive ERC R_2 signal.

nm photoconverting flashes of the meta-II state, subsequent 500 nm flashes produce normal ERCs with only R_2 (Figure 3D). These signals are consistent with prior measurements of meta-II photoconversion with both the early receptor potential and ERC techniques (*12*, *21*). Derivatives of the photoconversion waveforms (as in Figure 3A,C) show opposing early components but comparable slow millisecond-order inward relaxing components (not shown).

DISCUSSION

The reaction of all-*trans*-retinal with HEK293S cells (no opsin) supports a purely negative charge motion which is quenched by NH_2OH in the dark. The action spectrum of this charge motion is consistent with the formation of PSB pigments (λ_{max} = 440 nm) (*16*) with lipids or non-opsin proteins in the plasma membrane surface to yield an oriented population of chromophores. A significant bathochromic shift and spectral broadening of the negative charge motion action spectrum of all-*trans*-retinal-regenerated WT HEK293S giant cells occurs relative to that found in HEK293S giant cells. This "opsin shift", seen in both the absolute and difference action spectra, indicates that all-*trans*-retinal undergoes a specific reaction with the human rod opsin apoprotein in the plasma membrane of WT HEK293S giant cells to form a population of PSBs. Compared to the action spectrum obtained from HEK293S giant cells, the spectral broadening found in the WT HEK293S action spectrum suggests that all-*trans*-retinal is forming *additional* PSBs in a unique environment. Retinal will only form PSBs with primary amines, and since the only qualitative difference between the plasma membranes of WT HEK293S and HEK293S giant cells is the presence of human rod opsin apoprotein in the former, the site of reaction of all-*trans*-retinal with human rod opsin in WT HEK293S cells is constrained to lysine residues of the apoprotein which reside within or adjacent to the membrane bilayer where they could contribute to transmembrane charge motions. Lysine residues localized well away from the insulating membrane dielectric bilayer, for example, in loops connecting transmembrane α-helices, are unlikely to contribute to the ERC charge motions we have measured. Such side chains would likely be more unconstrained and isotropically distributed and reside outside the charge screen layer of the membrane at the instant of flash photolysis. These conditions would both obviate a transmembrane current with a purely negative polarity and disperse charge redistribution within the aqueous environment rather than promote a net transmembrane capacitative current. As in bovine rod opsin, there are 10 nonessential lysine residues in the human rod opsin apoprotein and one "essential" lysine residue at K296, which is the site of formation of the buried protonated Schiff base with 11-*cis*-retinal that forms the chromophore of rhodopsin (*22*, *23*). Where does all-*trans*-retinal react in the opsin apoprotein environment? The lysine that reacts with all-*trans*-retinal in human rod opsin must be in a fairly unique environment which (a) induces a charge delocalization along the all-*trans*-retinylidene chromophore to bathochromically shift the PSB absorption, (b) provides some protection against attack by NH_2OH, and (c) supports prompt photoconversion, upon near-UV photolysis, to a ground state visible-absorbing pigment with a *cis*-retinylidene chromophore that supports R_2 charge motions.

The opsin apoprotein protects bound all-*trans*-retinal from reaction with NH_2OH in the dark. Is the mechanism similar to how rhodopsin protects its 11-*cis*-retinylidene chromophore from NH_2OH attack in the dark? We considered two models by which the NH_2OH-resistant negative signal could arise in WT HEK293S cells upon visible flash photolysis. all-*trans*-Retinal could form PSBs with the K141, K231, or K311 side chains which are the only lysines in human (or bovine) opsin that are localized in a low dielectric environment of the cytoplasmic membrane surface near the termini of the third, fifth, and seventh transmembrane helices, respectively (*24*, *25*). Other lysine residues in the cytoplasmic loops are likely to be too remote from the membrane to contribute to transmembrane ERC charge motion or too exposed to protect against aqueous NH_2OH attack. If all-*trans*-retinal formed a PSB at K141, K231, or K311, then the polyene component and β-ionone ring would, necessarily, be buried within the low dielectric environment of the opsin protein in order to obtain the bathochromically shifted (above 440 nm) broad action spectrum found in WT HEK293S cells (Figure 2A). In the first model we consider PSB formation between all-*trans*-retinal and either K141, K231, or K311 and with the β-ionone ring docked in its native site in the ligand binding pocket. Molecular graphic models of the ground state of rhodopsin (*26*−*28*) and the recent crystal structure (*29*) indicate that the polyene chain (C6−C15) of all-*trans*-retinal is insufficiently long (by 10−20 Å) to

support PSB formation with the primary amines of the K141, K231, or K311 side chains. However, we do not exclude the possibility that additional docking sites for the β-ionone ring, other than within the native ligand binding pocket, will be identified. An alternative model for NH_2OH protection therefore appears more likely. all-*trans*-Retinal would be protected from NH_2OH by entering the 11-*cis*-retinal binding pocket of opsin and forming a PSB with K296, the native chromophore attachment site (*1*) and the only lysine residue in opsin that is physically located internal to the membrane−solution interfaces (*3*). This leads us to the tacit conclusion that, after the β-ionone ring docks in its native binding site, the all-*trans*-retinal polyene chain is structurally accommodated into the normal ligand binding pocket of human rod opsin due to structural flexibility that was not previously appreciated. This could permit PSB formation with K296 and an incomplete opsin shift due to conformational variations induced in the chromophore and counterion environments by accommodating the all-*trans* chromophore.

The ERC responses of all-*trans*-retinal-regenerated WT HEK293S giant cells to near-UV photolysis also provide insight into the location of the reactive site in normal human opsin. What pigment-forming mechanisms could support 350 nm charge motion responses? They could result from (a) membrane-solubilized, and oriented, free all-*trans*-retinal dipoles or unprotonated SBs formed with specific membrane lipids or non-opsin proteins, (b) a nonconcovalent complexation and orientation of all-*trans*-retinal within a ligand binding pocket, or (c) unprotonated SBs formed with membrane-buried lysine side chains of opsin either near the cytoplasmic membrane surface (i.e., K141, K231, K311) or at K296 in the native pocket. Near-UV absorbing pigments resulting from (a) can be excluded because they would be otherwise identical between WT HEK293S and HEK293S cells, but HEK293S cells regenerated with all-*trans*-retinal do not have 350 nm ERC responses.

To distinguish between mechanisms b and c, we considered both dipole transitions and proton exchange mechanisms. The initial positive component of the 350 nm charge motion (≤ 1 μs) in all-*trans*-retinal-regenerated WT HEK293S cells could be due to dipole reorientation of retinal in opsin resulting from photochemical isomerization (picosecond) or slower (nanosecond to microsecond) thermal transitions. We compared the polarity of ERC signals from our measurements with a model for chromophore dipole transitions in rhodopsin determined from time-resolved linear dichroism studies (*30*). Dipole moment transitions at peak absorption of the states from lumirhodopsin$_{497nm}$ → metarhodopsin-I$_{478nm}$ → meta-II$_{380nm}$, or reverse transitions from these states, are inconsistent with the polarity of the ERC signals measured from WT HEK293S cells regenerated with all-*trans*-retinal and stimulated with near-UV (or visible) flashes. Therefore, we conclude that dipole moment transitions of the chromophore cannot explain the fast positive or negative charge motions observed in response to 350 or 500 nm stimuli, respectively. Dipole movements of charged or polarizable opsin side chains, or additional state transitions overlapping with the flash duration ($\approx$14 μs), cannot be explicitly ruled out, however. Proton movements are known to occur in vertebrate rhodopsin on a broad time scale (microsecond to millisecond) (*31*, *32*). If all-*trans*-retinal entered the native ligand binding pocket of opsin and formed an unprotonated SB and a meta-II-like state, then the different phases of the 350 nm response (Figure 3A) could be explained by a mechanistic model. For a positive charge motion caused by proton movement the charge transfer must be directed vectorially outward across the membrane. Since the E113 side chain resides close to the extracellular membrane surface of rhodopsin above the retinylidene linkage, the rapid microsecond-order rise time of the positive 350 nm response could represent the release of a proton on E113-H to the extracellular solution and the electrostatically neutralizing reprotonation of the SB from an internal residue. The shift from the rapid positive to the slow negative (inward) charge response (10−100 ms) upon 350 nm photolysis could be explained by a vectorial deprotonation of side chains (e.g., E134-H), located near the intracellular surface of rhodopsin, into the cytoplasm to yield a slow inward current. These proton transfers would reverse the known events that lead to meta-II formation while reconstituting the titration of critical residues (e.g., PSB^+-H, $E113^-$, $E134^-$) that are necessary for a stable ground state that does not signal transducin. We proposed a similar model for the inverted and similar charge motions seen upon near-UV photolysis of the meta-II state which was populated by forward bleaching of the ground state of rhodopsin (see ref *12*). In that model photoconversion of meta-II to rhodopsin occurs by the reversal of known proton exchange reactions which likely underlie the normal R_2 signal generated during *forward* bleaching of rhodopsin to meta-II, that is, vectorially outward Schiff base proton transfer to the counterion $E113^-$ and proton uptake from the cytoplasm to titrate accessible side chains buried near the intracellular surface of rhodopsin (e.g., $E134^-$). In stark contrast, it would be highly unlikely for a noncovalent complex (mechanism b) to manifest directed proton exchange and resist NH_2OH extraction in darkness. Thus mechanism c is most consistent with our 350 nm data provided that the SB forms with K296 in the native ligand binding pocket of opsin. The ERC responses to both visible and near-UV flashes then can be explained as charge motions resulting from those fractions of pigments with protonated and unprotonated Schiff bases, respectively, with an all-*trans*-retinylidene chromophore at K296. Even though diffusion of retinaldehydes into the native ligand pocket of opsin is predictably fast, the kinetics of both hydrolysis and reformation of PSBs are slow (minutes) (*12*, *35*). These rate-limiting reactions would appear to preclude detection of normal (*cis*-retinylidene PSB) ERCs to 500 nm flashes, given only seconds after 350 nm photoconversion, if an all-*trans*-retinylidene SB, or a noncovalent complex, was photoisomerized anywhere else in opsin (or another protein) and then had to hydrolyze, diffuse, dock, and re-form a *cis*-retinylidene PSB in the native ligand binding pocket with K296. We therefore conclude that the 350 nm charge motion responses to all-*trans*-retinal-regenerated WT HEK293S giant cells result from chromophore that has docked and reacted in an environment within immediate proximity to the native ligand binding pocket of opsin.

How do our findings compare with observations made in prior studies? Noncovalent complexes of all-*trans*-retinal with bovine opsin were proposed when spectrophotometric measures were unable to detect pigment formation with opsin (*9*, *10*). Noncovalent interactions of all-*trans*-retinal with opsin would not, however, form visible-absorbing pigments

because a major portion of the spectral shift between free retinal and a PSB is the protonation of the covalent linkage (*36*). We demonstrate here that all-*trans*-retinal, while clearly forming a PSB with human opsin, yields a visible-absorbing pigment that lacks the normal capacity to support R_2 (and hence meta-II_{380nm}) upon 500 nm flash photolysis (*11*, *12*, *37*). Hence, at a minimum, the environment around the all-*trans*-retinylidene chromophore is distinct from that found in rhodopsin with its 11-*cis*-retinylidene chromophore. Noncovalent complexes would be unlikely to promote charge motions in the ERC assay. The prior lack of detection by absorption spectrophotometry of pigments resulting from covalent association between all-*trans*-retinal and the native binding pocket of opsin (*9*, *10*, *36*) can be explained if (a) the visible absorbing state(s) has (have) low extinction coefficients, (b) the absorption of such pigments overlaps spectrally with the absorption of free chromophore (e.g., unprotonated Schiff bases), (c) the vectorial orientation of the absorption dipole established upon PSB formation with all-*trans*-retinal is orthogonal to the membrane plane and hence is more readily detected by transmembrane charge motions than spectrophotometry, and (d) the comparative sensitivity and unique properties of the ERC measurement, when compared to spectrophotometry, allow these states to be identified.

In summary, this study provides strong evidence that all-*trans*-retinal forms both protonated and unprotonated Schiff bases within the human rod opsin apoprotein at a site(s) which remain(s) to be determined but most likely involves the native ligand binding pocket and K296. A noncovalent ligand binding pocket for all-*trans*-retinal has recently been identified near the palmitoylated cysteines, but this site cannot be the one that we have identified because, in contrast to our measures (Figure 3), photoregeneration does not occur from retinal coupled in this environment (*38*). The all-*trans*-retinal-induced charge motions are unique in comparison to the 11-*cis*-retinal ERC signals, and in fact, it is now possible to separate these negative and positive signals for independent analysis in rhodopsin charge motion studies. The ERC approach offers a sensitive means to investigate all-*trans*-retinal−opsin interactions which have important physiological consequences, even if present in low stoichiometry. Our ERC data and model may shed light on the mechanism of how the binding of all-*trans*-retinal by rod opsin leads to a meta-II-like state that both activates transducin turnover and promotes carboxyl-terminal phosphorylation by rhodopsin kinase (*6*−*10*, *33*, *34*). It may be that protons are taken up into the cytoplasmic face of opsin upon occupation of the native ligand pocket by all-*trans*-retinal *and* SB formation, similar to the critical protonation events during forward bleaching that lead to the biochemically active state. This work suggests that the opsin apoprotein is a receptor for both the antagonist (11-*cis*-retinal) and agonist (all-*trans*-retinal) ligands, a result which is consistent with the broad G-protein-coupled heptahelical receptor family. The conformational flexibility of the binding pocket of human rod opsin toward all-*trans*-retinal does not appear to be as restrictive as initially proposed for bovine opsin (*39*−*41*) but rather more consistent with contemporary views of protein conformational landscapes and a multiplicity of intermediate states. The implicit adaptability of the ligand pocket of human rod opsin suggests that ERC studies of analogue rhodopsins regenerated with a battery of synthetic chromophores could be a productive means to investigate the molecular biophysics and dynamics of conformational state changes in rhodopsin along the paths of both photoactivation and photoreversal.

ACKNOWLEDGMENT

We thank Dr. Jeremy Nathans (Johns Hopkins Medical School) for providing the WT HEK293S cell line, Dr. Bruce Stillman (Cold Spring Harbor Laboratories) for providing the parent untransfected HEK293S line, and Dr. Rosalie Crouch (Medical University of South Carolina) and the National Eye Institute for providing 11-*cis*-retinal. We thank Drs. Robert R. Birge, Kenneth W. Foster, and Barry E. Knox for stimulating scientific discussions during the progress of this work and a critical review of the manuscript by Drs. Robert Birge, Kenneth Foster, and Bryan Vought prior to its submission.

REFERENCES

1. Bownds, D. (1967) *Nature 216*, 1178−1181.
2. Birge, R. R. (1990) *Biochim. Biophys. Acta 1016*, 293−327.
3. Baldwin, J. M. (1993) *EMBO J. 12*, 1693−1703.
4. Fukuda, Y., and Yoshizawa, T. (1981) *Biochim. Biophys. Acta 675*, 195−200.
5. Cohen, G. B., Yang, T., Robinson, P. R., and Oprian, D. D. (1993) *Biochemistry 32*, 6111−6115.
6. Surya, A., Foster, K. W., and Knox, B. E. (1995) *J. Biol. Chem. 270*, 5024−5031.
7. Buczylko, J., Saari, J. C., Crouch, R. K., and Palczewski, K. (1996) *J. Biol. Chem. 271*, 20621−20630.
8. Surya, A., and Knox, B. E. (1997) *J. Biol. Chem. 272*, 21745−21750.
9. Jager, S., Palczewski, K., and Hofmann, K. P. (1996) *Biochemistry 35*, 2901−2908.
10. Surya, A., and Knox, B. E. (1998) *Exp. Eye Res. 66*, 599−603.
11. Sullivan, J. M., and Shukla, P. (1999) *Biophys. J. 77*, 1333−1357.
12. Shukla, P., and Sullivan, J. M. (1999) *J. Gen. Physiol. 114*, 609−636.
13. Sullivan, J. M., Brueggemann, L., and Shukla, P. (2000) *Methods Enzymol. 315*, 268−293.
14. Sullivan, J. M. (1998) *Rev. Sci. Instrum. 69*, 527−539.
15. Makino, C. L., Taylor, W. R., and Baylor, D. A. (1991) *J. Physiol. 442*, 761−780.
16. Kito, Y., Suzuki, T., Azuma, M., and Sekoguti, Y. (1968) *Nature 218*, 955−957.
17. Nobamoto, N., and Tien, H. T. (1971) *Biochim. Biophys. Acta 241*, 129−146.
18. Zhukovsky, E. A., and Oprian, D. D. (1989) *Science 246*, 928−930.
19. Sakmar, T. P., Franke, R. R., and Khorana, H. G. (1989) *Proc. Natl. Acad. Sci. U.S.A. 86*, 8309−8313.
20. Nathans, J. (1990) *Biochemistry 29*, 9746−9752.
21. Cone, R. A. (1967) *Science 155*, 1128−1131.
22. Nathans, J., and Hogness D. S. (1984) *Proc. Natl. Acad. Sci. U.S.A. 81*, 4851−4855.
23. Longstaff, C., Calhoon, R. D., and Rando, R. R. (1986) *Biochemistry 25*, 6311−6319.
24. Abdulaev, N. G., and Ridge, K. D. (1998) *Proc. Natl. Acad. Sci. U.S.A. 95*, 12854−12859.
25. Altenbach, C., Yang, K., Farrens, D. L., Farahbakhsh, Z. T., Khorana, H. G., and Hubbell, W. L. (1996) *Biochemistry 35*, 12470−12478.
26. Lin, S. W., Imamoto, Y., Fukada, Y., Shichida, Y., Yoshizawa, T., and Mathies, R. A. (1994) *Biochemistry 33*, 2151−2160.
27. Herzyk, P., and Hubbard, R. E. (1995) *Biophys. J. 69*, 2419−2442.
28. Shieh, T., Han, M., Sakmar, T. P., and Smith, S. O. (1997) *J. Mol. Biol. 269*, 373−384.

29. Palczewski, K., Kumasaka, T., Hori, T., Behnke, C. A., Motoshima, H., Fox, B. A., Le Trong, I., Teller, D. C., Okada, T., Stenkamp, R. E., Yamamoto, M., and Miyano, M. (2000) *Science 289*, 739−745.
30. Lewis, J. W., and Kliger, D. S. (1992) *J. Bioenerg. Biomembr. 24*, 201−210.
31. Arnis, S., and Hoffman, K. P. (1993) *Proc. Natl. Acad. Sci. U.S.A. 90*, 7849−7853.
32. Dickopf, S., Mielke, T., and Heyn, M. P. (1998) *Biochemistry 37*, 16888−16897.
33. Cohen, G. B., Oprian, D. D., and Robinson, P. R. (1992) *Biochemistry 31*, 12592−12601.
34. Arnis, S., and Hofmann, K. P. (1995) *Biochemistry 34*, 9333−9340.
35. Cusanovich, M. A. (1982) *Methods Enzymol. 81*, 443−447.
36. Hubbard, R., and Sperling, L. (1973) *Exp. Eye Res. 17*, 581−589.
37. Cafiso, D. S., and Hubbell, W. L. (1980) *Biophys. J. 30*, 243−264.
38. Sachs, K., Maretzki, D., Meyer, C. K., and Hofmann, K. P. (2000) *J. Biol. Chem. 275*, 6189−6194.
39. Hubbard, R., and Wald, G. (1952) *J. Gen. Physiol. 36*, 269−315.
40. Matsumoto, H., and Yoshizawa, T. (1978) *Vision Res. 18*, 607−609.
41. Liu, R. S. H., Matsumoto, H., Kini, A., Asato, A. E., Denny, M., Kropf, A., and DeGrip, W. J. (1984) *Tetrahedron 40*, 473−482.

BI002267G